Phase separation near the Mott transition in $La_{2-x}Sr_xCuO_4$

1990 J. Phys.: Condens. Matter 2 665

(http://iopscience.iop.org/0953-8984/2/3/015)

J. Phys.: Condens. Matter **2** (1990) 665–676. Printed in the UK

Phase separation near the Mott transition in $La_{2-x}Sr_xCuO_4$

R S Markiewicz

Physics Department, Northeastern University, Boston, MA 02115, USA† and
Department of Physics, Boston University, Boston, MA 02215, USA

Received 19 July 1989

Abstract. Competition between the Mott transition and Fermi surface nesting in a $Cu–O_2$ plane is studied in the limit of infinite on-site Coulomb repulsion . By incorporating direct O–O hopping, the nesting condition (Fermi surface at van Hove singularity) can be shifted away from half filling. The Mott transition (actually a transition to a charge transfer insulator) remains at half filling, driven by electron correlation effects, herein described via a slave boson formalism. Away from half filling, electron–phonon coupling leads to a phase separation into the insulating phase near half filling, and a metallic phase close to the van Hove singularity. The consequences of this phase separation for high-T_c superconductivity are briefly discussed.

1. Introduction

In the new, high-T_c superconducting oxides, typefied by $La_{2-x}Sr_xCuO_4$ (LSCO) and $YBa_2Cu_3O_{7-\delta}$ (YBCO), there is an intimate competition between an insulating, antiferromagnetic phase and the metallic, superconducting phase. Since the insulating phase occurs close to half filling of the $Cu–O_2$ antibonding band ($x \simeq 0$ for LSCO), it is believed that this phase is produced by strong electron correlation effects (on-site Coulomb repulsion, U). Modelling this competition theoretically has proven difficult. One approach is to start with a model of the antiferromagnetic insulator, and then study the effect of doping it with additional holes. Alternatively, a number of groups [1–3] have incorporated correlation effects into a Fermi liquid picture, via a slave boson formalism [4–6]. This procedure, initially developed to describe intermediate valence and heavy fermion compounds, introduces a boson on each Cu site to constrain the system against double site occupancy. Applying this formalism to the copper oxide superconductors, the insulating phase is found to be a charge transfer insulator [3], rather than a Mott–Hubbard insulator, in the notation of [7].

I have previously suggested [8] that structure in the density of states (DOS) plays an important role in high-T_c superconductivity. In particular, there should be a sharp peak in the DOS associated with the van Hove singularity (VHS), where the Fermi surface first intersects the Brillouin zone boundary and nesting is optimal. While the slave boson approach is ideally suited for analysing such effects, the previous models must be modified. Most [1, 3] have utilised a simplified band structure which requires the VHS to lie exactly at half filling, which disagrees with detailed band structure calculations. On the other hand, Newns *et al* [2] introduce a very complete band

† Permanent address.

0953-8984/90/010665+12$03.50

structure model, which is difficult to use in simple calculations. In this paper, I present a simple band structure model, suitable for slave boson calculations, in which the VHS can be arbitrarily positioned. The model is applied to two calculations. First, it is shown that shifting the DOS peak away from half filling has virtually no effect on the transition to an insulating phase. Secondly, it is shown that this DOS peak plays a very important role away from half filling. In particular, the VHS causes a minimum in the structural free energy, leading to an instability of the uniform phase (miscibility gap) in materials doped away from the VHS. As discussed elsewhere [8,9], this DOS peak also plays a much more direct role in high-T_c superconductivity.

The Cu–O_2-plane band structure is modelled by coupling three orbitals: the Cu $d_{x^2-y^2}$ and one p orbital from each of the two O atoms in the unit cell. The three bare band parameters are $\Delta E = E_{Cu} - E_O$, the difference between the Cu and the O energy levels; t_{CuO}, the Cu–O hopping matrix element; and t_{OO}, the O–O direct hopping element. The energy dispersion relations were discussed in [8]. For present purposes, it is sufficient to consider a two-band approximation:

$$E_k = \frac{\Delta E}{2} + \tilde{E}_p \pm \left[\left(\frac{\Delta E}{2} - \tilde{E}_p\right)^2 + 2t_{CuO}^2\gamma_k^2\right] \tag{1}$$

where $\gamma_k^2 = \sin^2(k_x a/2) + \sin^2(k_y a/2)$, $\tilde{E}_p = 2t_{OO}\sin(k_x a/2)\sin(k_y a/2)$, and a is the lattice constant. Figure 1 shows the resulting Fermi surface at half filling for several values of the parameters. Note that the centre of the Brillouin zone is chosen such that $k_x = k_y = 0$ corresponds to the top of the antibonding band (the M point in the usual Brillouin zone).

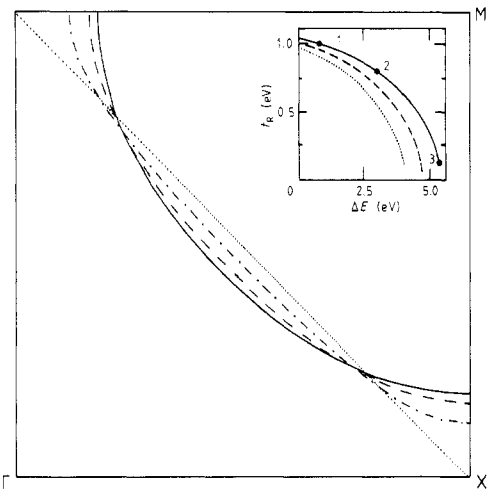

Figure 1. Renormalisation of the Fermi surface at half filling as a function of ΔE. Curves correspond to $n = 1$, $t_{OO} = 0.48$ eV, points in inset: full curve, 1; broken curve, 2; chain curve, 3. Dotted line is the Fermi surface for $t_{OO} = 0$, independent of t_R. Inset: renormalisation of t_{CuO} as a function of ΔE, for $t_{OO} = 0$ (dotted curve); 0.24 (broken curve); 0.48 eV (full curve).

On-site (Cu) Coulomb repulsion U is incorporated via the slave boson formalism [1–6]. The present calculation follows Kotliar, Lee and Read [1] (KLR). Inclusion

of the on-site Coloumb repulsion renormalises the parameters ΔE and t_{CuO}, shifting and narrowing the Cu band. The slave boson technique allows these effects to be incorporated by requiring the real d hole plus the boson to satisfy a sum rule which prevents double occupancy of the Cu orbital. In mean field, this sum rule becomes:

$$\sum_k u_k^2 f(E_k) + r_0^2 = \frac{1}{2} \tag{2}$$

where $f(E)$ is the Fermi function, r_0 is the mean-field amplitude of the slave boson, and u_k is the d-wave amplitude of the wavefunction. The chemical potential is chosen such that $2\sum_k f(E_k) = n = 1 + x$ in LSCO, where n is the number of holes per unit cell. The d-band renormalisation is given by

$$\Delta E_R - \Delta E = \frac{1}{r_0^2} \sum_k u_k^2 f(E_k)(\Delta E_R - E). \tag{3}$$

For given values of ΔE, t_{CuO} and t_{OO}, equations (2) and (3) are solved self-consistently to yield values of ΔE_R and r_0, or equivalently of the renormalised Cu–O hopping matrix $t_R = \sqrt{2}\, r_0 t_{CuO}$. The self-consistency arises because the renormalised parameters ΔE_R and t_R are used in the dispersion relation, (1) (t_{OO} is assumed to be unaffected by renormalisation).

If $t_{CuO} = 0$, the dispersionless d band is completely decoupled from a p band of width $4t_{OO}$ (recall that (1) ignores the bonding part of the Cu–O bands). For finite t_{CuO}, the renormalisation depends sensitively on the band filling. When $t_{OO} = 0$, an approximate analytical solution can be found [1]. For finite t_{OO}, the following results were evaluated numerically. In these calculations, the values of $t_{CuO} = 1.2$ eV, and $t_{OO} \simeq 0.0$–0.5 eV were chosen as approximately representative of LSCO, while ΔE was varied in the range 0–6 eV. The numerical calculations are restricted to $T = 0$, and are carried out by adjusting the values of t_R, ΔE_R until equations (2) and (3) reproduce the values of ΔE and t_{CuO}. There is always a solution to equations (1)–(3) with $r_0 = 0$, and this solution is assumed to hold when the numerical calculation fails to converge.

2. Insulating state at half filling

When $t_{OO} = 0$, the Fermi surface at half filling is square (dotted line in figure 1), leading to perfect nesting, which should drive a transition to an insulating phase. Letting t_{OO} differ from zero shifts the nesting condition away from half filling, figure 1, thereby allowing separation of the effects of nesting from those of double Cu occupancy. Figures 1–3 show that these latter correlations still drive a transition to an insulating state at half filling, if the ratio $\Delta E/t_{CuO}$ is large enough. For the present example, $t_{CuO} = 1.2$ eV, the bandwidth t_R is renormalised to approximately zero for $\Delta E \geq 4$–6 eV (inset, figure 1). This result depends only weakly on t_{OO}. The renormalised carriers have a large DOS at the Fermi level (figure 2), and hence a large effective mass, and the Fermi surface is renormalised in the direction of perfect nesting (figure 1). For small but finite t_R, the deviation of the Fermi surface from square is a function of $t_{OO}/\Delta E_R$, independent of t_R. This still decreases as ΔE increases, because ΔE_R is an increasing function of ΔE. However, if ΔE is large enough, $t_R = 0$ (inset, figure 1), so the dispersion becomes meaningless. As shown by KLR, the system passes over

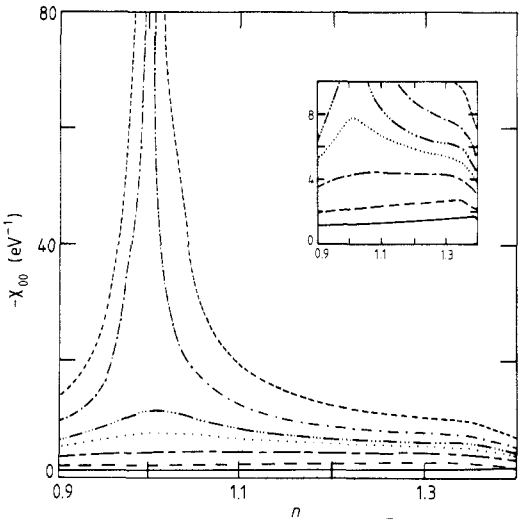

Figure 2. Renormalised susceptibility, $-\chi_{00}$, plotted against hole concentration for several values of ΔE with $t_{CuO} = 1.2$ eV, $t_{OO} = 0.48$ eV. In order of increasing χ, the curves correspond to $\Delta E = 2.4$, 3.6, 4.2, 4.4, 5.0, 5.4 and 6.0 eV. Inset: blow-up of low-χ_{00} data.

to a Néel ground state (charge transfer insulator) when the renormalised bandwidth becomes smaller than the superexchange constant, J.

Figure 2 shows the renormalised magnetic susceptibility, χ_{00}, as a function of n for various values of ΔE. Here,

$$\chi_{0q} = -\sum_k \frac{f(E_k) - f(E_{k+q})}{E_k - E_{k+q}} \tag{4}$$

For small values of ΔE and $t_{OO} \neq 0$, $-\chi_{00}$ has a weak peak at finite $n-1$, corresponding to the (renormalised) VHS. As ΔE increases, this peak turns into a shoulder. Meanwhile, a large peak grows at $n = 1$. Note the extreme sensitivity of this peak to ΔE, typical of a Kondo effect. The ground-state energy E_0 can be separated into a quasi-particle part $\langle E \rangle \equiv 2\sum_k f(E_k)E_k$ and a slave boson contribution $E_B = (\Delta E_R - \Delta E)(2r_0^2 - 1)$. Thus,

$$E_0 = \langle E \rangle + E_B. \tag{5}$$

The quasi-particle energy $\langle E \rangle$ shows a drop near half filling which becomes sharper as ΔE increases, and is discontinuous [1] when $t_R = 0$. This jump is a direct consequence of the infinite value of U. To avoid double hole occupancy of any Cu atom while maintaining $n > 1$ requires significant hybridisation with the O band. Hence, as n passes through 1, ΔE_R must shift from a value near ΔE to a value near zero [1]. However, this discontinuity is exactly cancelled by the term E_B, and, as $t_R \to 0$, E_0 develops a cusp at half filling, inset to figure 3. Because of this cusp, the insulating state is only energetically stable if it is impossible to form states with $n < 1$. This is true in LSCO, where $n < 1$ corresponds to Sr contents $x < 0$.

The values of the the band structure parameters I have employed are in good agreement with recent theoretical determinations of these values [10] for LSCO, as illustrated in table 1. The parameters can all be scaled by the same value, to bring

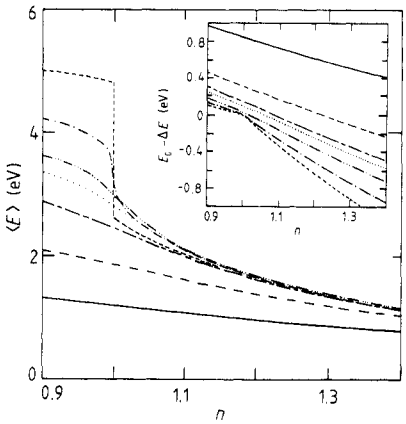

Figure 3. Average hole energy $\langle E \rangle$ plotted against hole concentration, for same parameters as in figure 2. Inset: $E_0 - \Delta E$, for same parameters.

t_{CuO} into exact agreement, but the parameter t_{OO} is fixed by the location of the VHS, while ΔE must be large enough to account for the transition to the insulating state at half filling, $\Delta E \simeq 3(t_{CuO} + t_{OO})$. The doping dependence of T_c does not precisely fix the value of x at the VHS, allowing a range $x \simeq 0.15$–0.2. The value of t_{OO} found in [10] produces an acceptable value, $x = 0.178$ at the VHS. (As mentioned above, the larger value of t_{OO} will cause ΔE to be larger by $\sim$ 0.4eV.) Whereas band structure calculations initially indicated that ΔE was small, Hybertsen *et al* [10] pointed out that these calculations already include correlation effects on average, and that the bare value of ΔE is considerably larger. Two theoretical values of ΔE are listed in table 1. This is because the present calculation does not explicitly consider the near-neighbour Coulomb repulsion parameter V, so the parameter ΔE should assume a value intermediate between the true ΔE and $\Delta E + 2V$. It is the latter value which controls the proximity of the system to the insulating phase [3]. This value is in good agreement with the values found in figures 2 and 3 at the onset of the sharp rise in $-\chi_0$. In the remainder of this paper, in particular in figures 4 and 5, I will incorporate the parameter values of [10].

Table 1. Energy band parameters.

Parameter	[10] and figures 4 and 5	Scaled† figures 2 and 3
t_{CuO} (eV)	1.3	1.3
t_{OO} (eV)	0.65	0.52
ΔE (eV)	(3.6)	
	6.0‡	5.4–5.8

† Using a scale factor $S = 1.083$. If all energies are multiplied by S and all susceptibilities and DOS divided by S, the results of figures 2,3 remain correct.
‡ Actually $\Delta E + 2V$, where V is the nearest-neighbour Coulomb repulsion.

The stability of the Fermi liquid state with respect to the antiferromagnetic insulator may be determined by comparing E_0 to the energy in the insulating state. This latter quantity may be approximately estimated from the mean-field result, $\Delta E_{AF} = -J(x)$. This overestimates ΔE_{AF} at room temperature, because there is no long-range order. However, there is a strong two-dimensional order, so the error should be relatively

small, of order $\sim T_N/2J \simeq 10\%$. Following [11],

$$J(x) = J + K'x + 8Jx^2 \tag{6}$$

where $K' = (K - 7J)/4$, and K is the ferromagnetic exchange constant, with $J \simeq 116$ meV and $K \simeq 2J$ [12]. Experimentally, the Néel phase is stable only to $x \simeq 0.02$. Using the band parameters of [10] (table 1), the energies of the two phases are equal at $x \simeq 0.028$, in good agreement with experiment.

3. The VHS

In this Fermi liquid approach, there is a striking difference between the electric and the magnetic response of the system. The magnetic response is controlled by the renormalised susceptibility function, equation (4) and figure 2. Near half filling, χ_{0q} is largest for q on the Brillouin zone boundary, as expected for an antiferromagnetic instability; as holes are introduced, the uniform susceptibility, χ_{00}, becomes dominant (figure 4), i.e. the holes favour ferromagnetic coupling.

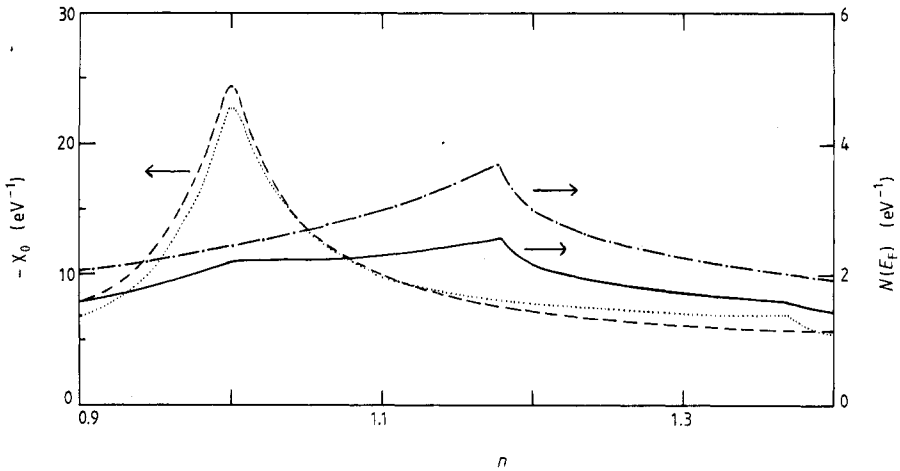

Figure 4. Magnetic susceptibilities χ_{00} (dotted curve) and $\chi_{0G_{10}}$ (broken curve), where G_{10} is the reciprocal lattice vector with $h = 1$, $k = 0$. Shown also are the bare DOS, $N_0(E_F)$ (chain curve), and the renormalised DOS, $N(E_F)$ (full curve). Parameters are $t_{CuO} = 1.3$ eV, $t_{OO} = 0.65$ eV, $\Delta E = 6.0$ eV.

The electric response is given by a very similar susceptibility function, only renormalised by Fermi liquid effects [13]:

$$\bar{\chi}_{0q} = \chi_{0q}/(1 + F_{0s}) \tag{7}$$

where $F_{0s} = m^*/m = -\chi_{00}/N_0(E_F)$, m^* is the renormalised mass, and $N_0(E_F)$ is the DOS of the unrenormalised bands. The renormalised DOS is given by $N(E_F) = -\bar{\chi}_{00}$. When $F_{0s} \gg 1$, this renormalisation produces a very striking result: whereas the magnetic response peaks at half filling, independent of t_{OO}, the electric response peaks at the VHS. For instance, as $F_{0s} \to \infty$, $N(E_F) \to N_0(E_F)$. Figure 4 contrasts the hole dependence of

χ_{00} and $\bar{\chi}_{00}$, showing that the latter peaks at the same hole density as $N_0(E_F)$. Both N_0 and N have a weak divergence at the VHS. For $t_{OO} = 0$, both diverge as $\log^2(E)$, but more weakly, $\sim \log(E)$, for $t_{OO} \neq 0$. To keep the DOS values finite, they are broadened in energy by 20 meV. This is of the magnitude expected for the combined effects of thermal and disorder broadening and c axis dispersion [8].

The Fermi liquid correction has a number of important consequences. For instance, in a one-dimensional metal χ and $\bar{\chi}$ diverge at the same time, leading to a competition between CDW, spin density wave (SDW), singlet superconducting (SS) and triplet superconducting (TS) instabilities. In the present two-dimensional model, these divergences are well separated, with SDW and TS instabilities associated with half filling and CDW and SS occurring at the VHS. (For simplicity, I label the phase in which the VHS coincides with the Fermi level as the VHS phase.) I have previously suggested [8] that high-T_c superconductivity is associated with a competition between CDW and SS formation, just as in the A15 compounds, and, indeed, in the $BaPb_{1-x}Bi_xO_3$ system.

Moreover, the peak in charge susceptibility confers a special stability on the VHS phase. There is a minimum in the structural free energy at this composition. Hence, materials doped away from this composition may be structurally unstable (miscibility gap), breaking up into a two-phase mixture with one phase at the VHS concentration. This stabilisation arises through the electron–ion interaction, in a manner similar to the Freidel model [14] for three-dimensional Hume–Rothery phases [15]. Within the present model, this stabilisation can be calculated using standard results for a pseudopotential theory which has been applied to a number of Cu bronzes [16]. These previous applications have, however, involved nearly free (s, p) electron susceptibilities, rather than the tight-binding bands used here. In analysing the total free energy of the coupled electron–ion system of the alloy, it is found that the structure sensitive part of the free energy is dominated by a single term

$$\Delta f_{str} = \frac{n}{2} \sum\nolimits'_G \bar{\chi}_G |v(G)|^2 \tag{8}$$

where Δf_{str} is the structural free energy per ion, n the ionic density, $v(G) = 4\pi e^2/\varepsilon G^2$, $\varepsilon \simeq 6.5$ is the dielectric constant, G a reciprocal lattice vector, the prime on the summation means $G \neq 0$, and $\bar{\chi}_G$ is the susceptibility

$$\bar{\chi}_G = \bar{\chi}_{0G}/(1 - v(G)\bar{\chi}_{0G}). \tag{9}$$

Applying this to a CuO_2 plane, the periodicity of the tight binding bands ensures that $\bar{\chi}_{0G}$ has the same value for each G in the original ('tetragonal') lattice. For a reciprocal lattice vector of the 'orthorhombic' $\sqrt{2} \times \sqrt{2}$ superlattice, $G_{hk} = (h+k, h-k)\pi/a$, there are two susceptibilities, $\bar{\chi}_0^o$ and $\bar{\chi}_0^e$ depending on whether $h+k$ is odd or even. Figure 5 plots the free energy per hole $F = (E_0 - \Delta E + \Delta f_{str})/n$, using the same parameters as figure 4 [10], with $\Delta E = 6.0$ eV. The broken curve in figure 5 shows the energy lowering near half filling produced by the antiferromagnetic insulating state, equation (6).

Stability of the various phases can be determined from figure 5 by using a standard tangent construction technique (dotted line). Since this dotted line falls below the free energy curve over a certain range of n values, a homogeneous material prepared at that composition will be unstable with respect to a heterogeneous mixture of the two phases corresponding to the end points of the dotted line, with the relative proportions determined by a lever rule. Note that this construction again assumes that states with $n < 1$ are physically inaccessible. Figure 5 clearly shows that a two-phase decomposition

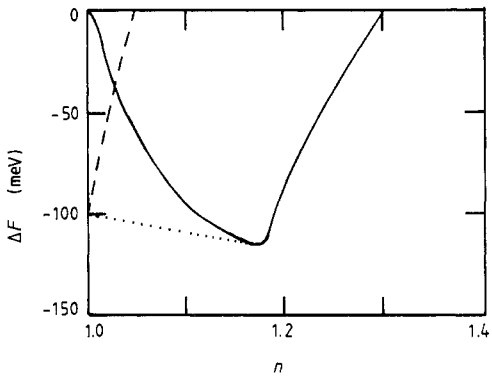

Figure 5. Average structural free energy $\Delta F = F(n) - F(1) + 1.965(n-1)$ eV (full curve) plotted against hole concentration. The broken line is the estimated modification due to antiferromagnetic phase. The dotted line shows free energy lowering due to two-phase coexistence. Note that a term linear in $(n-1)$ has been added to ΔF to remove an uninteresting monotonic contribution. This term has no effect on the tangent construction. Parameters are as in figure 4.

should occur both at higher dopings than the VHS, and near half filling. This implies that *the uniform state is unstable away from the van Hove singularity*, thus confirming an earlier prediction [17]. The value of the two-phase stabilisation energy, $\sim$ 60 meV, is comparable to those found in conventional Hume–Rothery phases [14–16].

Note that the details of the phase separation between half filling and the VHS are sensitive to the precise form of f_{str}, and hence may be somewhat different from figure 5. Thus, in figure 8 of [8a], the free energy was calculated using the bare DOS, $N_0(E_F)$, rather than the properly renormalised value, $N(E_F)$. While these two functions are similar, figure 4, the differences are sufficient to modify the range over which the uniform phase is unstable. Other contributions to the free energy (e.g. free energy of mixing of Sr or excess O) may also affect this instability. These contributions are likely to be monotonic in n (insensitive to the VHS), and hence have only a small effect. Thus, any contribution which is linear in n will have absolutely no effect on the phase transition. However, the (unknown) sign of the curvature of the residual terms is important, and these terms can expand or decrease the range over which the instability occurs.

4. Discussion

These results can most directly be applied to the LSCO family of superconductors. A similar picture presumably applies to YBCO as a function of oxygen deficiency δ, although complications arise due to oxygen vacancy ordering and possible carrier transfer to the Cu–O chains. So far, an insulating phase similar to La_2CuO_4 or $YBa_2Cu_3O_6$ has not been reported for the Bi or Tl families of superconductors. Near half filling, LSCO is an antiferromagnetic insulator. This is compatible with $\Delta E \geq 5$ eV, causing $t_R = 0$ and an instability to a commensurate spin-density wave.

Away from half filling ($x > 0$), there is considerable experimental evidence [8, 18, 19] that the material is a two-phase mixture away from $x = 0.15$. It is not clear that these two phases involve Sr segregation, which is limited by the slow Sr diffusion rate. Instead,

there may be a purely electronic phase separation, as in the ferron phase of magnetic semiconductors [20]. However, an excess of holes in LSCO may also be achieved by adding excess O. In this case, a well defined two-phase regime is formed [21], thanks to the fast O diffusion. For $x > 0.15$, the equilibrium state seems to involve two chemically distinct phases, although a metastable uniform state can be quenched in [18]. These results are consistent with figure 5, as discussed above. The properties of a purely electronic two-phase system are briefly described in the Appendix.

The nature of the transition into the heterogeneous phase depends on the curvature of the free energy as a function of n. For positive curvature ($d^2F/dn^2 > 0$), as at, e.g., $n = 1.1$ in figure 5, the free energy of the homogeneous phase is *locally* a minimum, so there is a barrier towards nucleating the stable heterogeneous phases. On the other hand, for negative curvature, as at $n = 1.2$ in figure 5, the free energy is locally a maximum, so no nucleation is required, and the material spontaneously phase separates (spinodal decomposition). While the present result seems to be in accord with experiment (it is easier to quench in a uniform phase for n below the VHS peak), the model is probably too simple to accurately predict the curvature of the free energy. This will be sensitive to certain omitted terms, such as the entropy of mixing. Since the nucleation barrier for a purely electronic phase separation will be small, these distinctions will not modify the calculations of the Appendix.

The sharp minimum in figure 5 is suggestive of a d-wave version of a heavy-fermion system, with the Fermi level pinned at a peak in the density of states. This picture is supported by optical reflectivity studies [22]. Millis and Lee [5] found that the slave bosons contribute a characteristic optical conductivity to heavy fermions. This term has the Fermi liquid form, $\sigma_b^{-1} \sim \omega_1^2 \equiv \omega^2 + (\pi k_B T/\hbar)^2$. The same result should hold in the present case, except that near the VHS, $\sigma_b^{-1} \sim \omega_1$ [23]. This is precisely the result found experimentally [22]. However, this interpretation of the optical results is not universally accepted. The interested reader should consult [24].

The consequences of these results for high-T_c superconductivity are important. From figures 1–3, it can be seen that the nature of the insulating transition is nearly independent of band structure effects (value of t_{OO}), whereas the nature of the electronic states away from half filling (e.g. DOS) depends sensitively on t_{OO}. LSCO is a two-phase mixture for $x > 0$, and the superconductivity is specifically associated with the phase at $x = 0.15$. Thus, a correct theory of high T_c superconductivity must properly describe this phase. Since all band structure information is lost at half filling, it will be particularly difficult to construct a model which smoothly extrapolates to the superconducting state, starting from the $x = 0$ state.

In the present calculations, it has been assumed that the unrenormalised band parameters ΔE, t_{CuO}, t_{OO}, are independent of n. This is not necessarily the case [25], but the additional complications do not seem to add any new physics.

The large susceptibility peak (figure 4) is indicative of a strong electron–phonon coupling in these materials. Enhancement of electron–phonon coupling near a two-dimensional van Hove singularity has been noted previously [26], and can lead to an additional enhancement of the DOS peak [27]. For a one-dimensional metal, the combination of strong on-site repulsion and charge density wave instability would normally not occur. However, interchain coupling (equivalent to $t_{OO} \neq 0$) strongly enhances the probability of such a combination [28].

In summary, strong electron correlation renormalises Fermi surface effects and structure in the density of states, but only weakly. The main effect of correlations lies in the magnetic response, producing a large peak in the magnetic susceptibility

at half filling, which can drive a transition to an antiferromagnetic insulating phase. The competition between a peak in the magnetic response at half filling and a peak in electric response away from half filling can lead to an instability of the uniform phase at intermediate dopings. Nevertheless, the superconductivity is associated predominantly with the peak in the density of states, as is clear from an analysis of the doping dependence of T_c [9].

Acknowledgments

This manuscript has greatly benefitted from the comments of two referees.

Appendix. Electronic instability

Even if the slow rate of Sr diffusion allows a uniform Sr distribution to be quenched in, the convex nature of the free energy curve should still drive a purely electronic instability, with the holes spontaneously separating into two phases. This means that the domains will be electrically charged, so that charging effects will limit the extent of phase separation to the microcrystalline regime, thus explaining the observation of proximity effects (dependence of T_c on x). In this Appendix, I give a rough estimate of the nature of this microcrystalline phase, generalising a similar calculation for the ferron phase in an antiferromagnetic semiconductor [20] to an array of two-dimensional discs.

The typical domain size is set by the competition between surface tension and charging effects. These energies in turn depend on the size and shape of the domains. For simplicity, I only consider an array of conducting ($x = x_c \simeq 0.178$) circular droplets in an insulating ($x = 0$) background, and the symmetric state of insulating droplets in a conducting background. I approximate the free energy of the uniform system (figure 5) by a parabola:

$$F_u = 4E_m x(x_c - x)/x_c^2 \tag{A1}$$

where $E_m \simeq 60$ meV. F_u is normalised such that the bulk energy within either type of domain, $x = 0$ or $x = x_c$, is zero. The surface tension is dominated by the excess kinetic energy associated with the non-uniform hole distribution, so the average interface energy per excess hole is

$$E_I = 5\pi E_F/16k_F R = \alpha/R \tag{A2}$$

where E_F (k_F) is the Fermi energy (wavenumber) of the holes. Defining the fraction of phase $x = x_c$ as $f_c = x/x_c$, and the fraction with $x = 0$ as $f_0 = 1 - f_c$, the charging energy can be shown to be [20]

$$E_c = \frac{\pi^2 e^2}{8\epsilon} n_{2d} R(1 + f_c - 2f_c^{1/2}) = \beta R \tag{A3}$$

where ϵ is the dielectric constant of the medium and n_{2d} is the two-dimensional hole density. Note that E_c vanishes when $f_c \to 1$. This is because Nagaev [20] approximated the unit cell as a sphere, so that as $f_c \to 1$ the domain just fills the unit cell. Hence, this

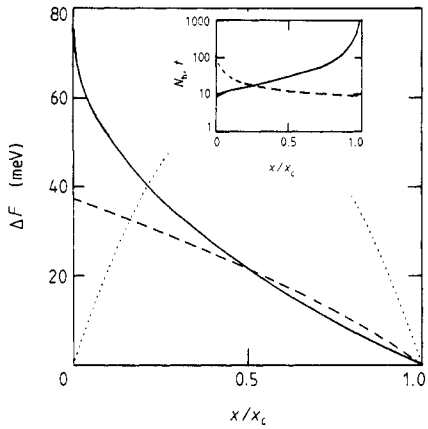

Figure 6. Free energy of inhomogeneous phases compared to that of uniform phase (dotted curve): the full curve is for metallic spheres in an insulating background; the broken curve for insulating spheres in a conducting background. Inset: equilibrium number of holes per conducting sphere (full curve) and grain boundary thickness parameter t (broken curve). The grain boundary thickness is $2t$, in Å.

phase is more appropriately thought of as a grain boundary phase, with a thin layer of insulator coating large grains of the metallic phase. The inset to figure 6 shows that the grain boundary thickness, $2t$, decreases by only $\sim 30\%$ as the doping increases from $x_c/2$ to x_c; over this same range, the number of holes per domain increases from 50 to ∞.

The equilibrium value of R is found by minimising the total energy of the two-phase system, $E_I + E_c$:

$$R^2 = \alpha/\beta. \tag{A4}$$

For the inverse phase with insulating domains in a conducting background, the equilibrium state can be found by symmetry, essentially interchanging f_c and f_0: thus, the equilibrium radius becomes just $R(1 - f_c)$, where $R(f_c)$ is the solution of (4), and the minimum energy is $(f_0/f_c)\Delta F(1 - f_c)$. Figure 6 shows that even with charging effects, these inhomogeneous phases have a lower free energy, except very close to $x = 0$. In this calculation a low-frequency dielectric constant $\epsilon \simeq 84$ was used [29]. The domain wall phase is found to have a lower free energy than the droplet phase. However, there may be a large kinetic barrier to forming an extended network of domain walls, so it may be possible to produce a metastable phase of droplets. The inset to figure 6 shows $N_h = n_{2d}\pi R^2$, the number of holes per droplet, and the grain boundary thickness, $2t$. For such small droplets, classical calculations cannot be quantitatively correct. Nevertheless, the calculation shows that charging effects by themselves are no barrier to phase separation. Since the droplets are so small, the randomly distributed Sr ions must play an important role, even in the absence of a classical phase separation.

The above calculations have neglected the problems of nucleating this phase. This is appropriate for a purely electronic phase separation, since the critical droplet radius is so small that any nucleation barrier is negligible.

These states are quite similar to the domain walls between antiferromagnetic regions discussed by Zaanen and Gunnarsson [30]. Moreover, similar electronic phases arise in

a number of situations, most (but not all) of which involve two-dimensionality. Thus, the scale of these domains is very similar to that found in the ferron phase [20]; a similar domain phase, found in association with two-dimensional Condon domains, may be relevant to the quantum Hall effect [31]. The domain wall phase could have some practical importance: the walls could act as intrinsic flux pinning centres, enhancing the value of the critical currents.

References

[1] Kotliar G, Lee P A and Read N 1988 *Physica* C **153–5** 538
[2] Newns D M, Pattnaik P C, Rasolt M and Papaconstantinopoulos D A 1988 *Physica* C **153–5** 1287; 1988 *Phys. Rev.* B **38** 7033 (1988)
Newns D M, Rasolt M and Pattnaik P C 1988 *Phys. Rev.* B **38** 6513
[3] Balseiro C A, Avignon M, Rojo A G and Alascio B 1989 *Phys. Rev. Lett.* **62** 2624
[4] Coleman P 1983 *Phys. Rev.* B **28** 5255
Read N and Newns D 1984 *Solid State Commun.* **52** 993
Auerbach A and Levin K 1987 *Phys. Rev. Lett.* **57** 877
[5] Millis A J and Lee P A 1987 *Phys. Rev.* B **35** 3394
[6] Newns D M and Read N 1987 *Adv. Phys.* **36** 799
[7] Zaanen J, Sawatsky G A and Allen J W 1985 *Phys. Rev. Lett.* **55** 418
[8] Markiewicz R S 1988 *Physica* C **153–5** 1181; 1989 *J. Phys.: Condens. Matter* **1** 8911, 8931
[9] Markiewicz R S and Giessen B C 1989 *Physica* C **160** 497
[10] Hybertsen M S, Schlüter M and Christensen N E 1989 *Phys. Rev.* B **39** 9028
[11] Aharony A, Birgeneau R J, Coniglio A, Kastner M A and Stanley H E 1988 *Phys. Rev. Lett.* **60** 1330
[12] Stechel E B and Jennison D R 1988 *Phys. Rev.* B **38** 4632
[13] Millis A J, Lavagna M and Lee P A 1987 *Phys. Rev.* B **36** 864
[14] Freidel J 1969 *Electron–Phonon Interactions and Phase Transitions* ed T Riste (New York: Plenum) p 1
[15] Heine V 1969 *The Physics of Metals* ed J M Ziman (Cambridge: Cambridge University Press) p 1
For a modern discussion of Hume–Rothery phases see ch 7.2 of Hafner J 1987 *From Hamiltonians to Phase Diagrams* (Berlin: Springer)
[16] Stroud D and Ashcroft N W 1971 *J. Phys. F: Met. Phys.* **1** 113
Evans R, Lloyd P and Mujibur Rahman S M 1979 *J. Phys. F: Met. Phys.* **9** 1939
Mujibur Rahman S M 1981 *J. Phys. F: Met. Phys.* **11** 1191
[17] Markiewicz R S 1987 *Mod. Phys. Lett.* B **1** 184
[18] Hinks D G, Dabrowski B, Zhang K, Segre C U, Jorgensen J D, Soderholm L and Beno M A 1988 *High-Temperature Superconductors* ed M Strongin *et al* (Pittsburgh: MRS) p 9
[19] Van Dover R B, Cava R J, Batlogg B and Rietman E A 1987 *Phys. Rev.* B **35** 5337
[20] Nagaev E L 1983 *Physics of Magnetic Semiconductors* (Moscow: Mir)
[21] Jorgensen J D, Dabrowski B, Pei S, Hinks D G, Sonderholm L, Morosin B, Schirber J E, Venturini E L and Ginley D S 1988 *Phys. Rev.* B **38** 11337
[22] Thomas G A, Orenstein J, Rapkine D H, Capizzi M, Millis A J, Bhatt R N, Schneemeyer L F and Waszczak J V 1988 *Phys. Rev. Lett.* **61** 1313
[23] Lee P A and Read N 1987 *Phys. Rev. Lett.* **58** 2691
[24] Markiewicz R S 1989 *Phys. Rev. Lett.* **62** 603
Millis A J and Thomas G A *Phys. Rev. Lett.* **62** 604
Timusk T and Tanner D B 1989 *Physical Properties of High Temperature Superconductors, I* ed D M Ginsberg (Singapore: World Scientific) p 339
[25] Freidel J 1969 *The Physics of Metals* ed J M Ziman (Cambridge: Cambridge University Press) p 340
[26] Zavaritsky N V 1984 *Physica* B **126** 369
[27] Kagan Yu and Prokof'ev N V 1987 *Zh. Eksp. Teor. Fiz.* **93** 366 (1987 *Sov. Phys.–JETP* **66** 211)
[28] Lee P A, Rice T M and Klemm R A 1977 *Phys. Rev.* B **15** 2984
Menyhard N 1977 *Solid State Commun.* **21** 495
[29] Sherwin M S, Richards P L and Zettl A 1988 *Phys. Rev.* B **37** 1587
[30] Zaanen J and Gunnarsson O 1989 *Phys. Rev.* B **40** 7391
[31] Markiewicz R S 1986 *Phys. Rev.* B **34** 4172, 4177